Supplemental material for

Large hemispheric difference in ultrafine aerosol concentrations in the lowermost stratosphere at mid and high latitudes

Christina J. Williamson[1,2], Agnieszka Kupc[2,3], Andrew Rollins[2], Jan Kazil[1,2], Karl D. Froyd[1,2], Eric A. Ray[1,2], Daniel M. Murphy[2], Gregory P. Schill[1,2], Jeff Peischl[1,2], Chelsea Thompson[1,2], Ilann Bourgeois[1,2], Thomas Ryerson[2*], Glenn S. Diskin[4], Joshua P. DiGangi[4], Donald R. Blake[5], Thao Paul V. Bui[6], Maximilian Dollner[3], Bernadett Weinzierl[3], Charles A. Brock[2]

[1]Cooperative Institute for Research in Environmental Sciences, University of Colorado, Boulder, CO 80309, U.S.A.
[2]Chemical Sciences Laboratory, National Oceanic and Atmospheric Administration, Boulder, CO 80305, U.S.A
[3]Faculty of Physics, Aerosol Physics and Environmental Physics, University of Vienna, 1090 Vienna, Austria
[4]NASA Langley Research Center, Hampton, VA 23681, USA
[5]Department of Chemistry, University of California Irvine, Irvine, CA 92697, U.S.A.
[6]Earth Science Division, NASA Ames Research Center, Moffett Field, California, U.S.A.

Correspondence to: Christina J. Williamson (christina.williamson@noaa.gov)

S1 LMS properties

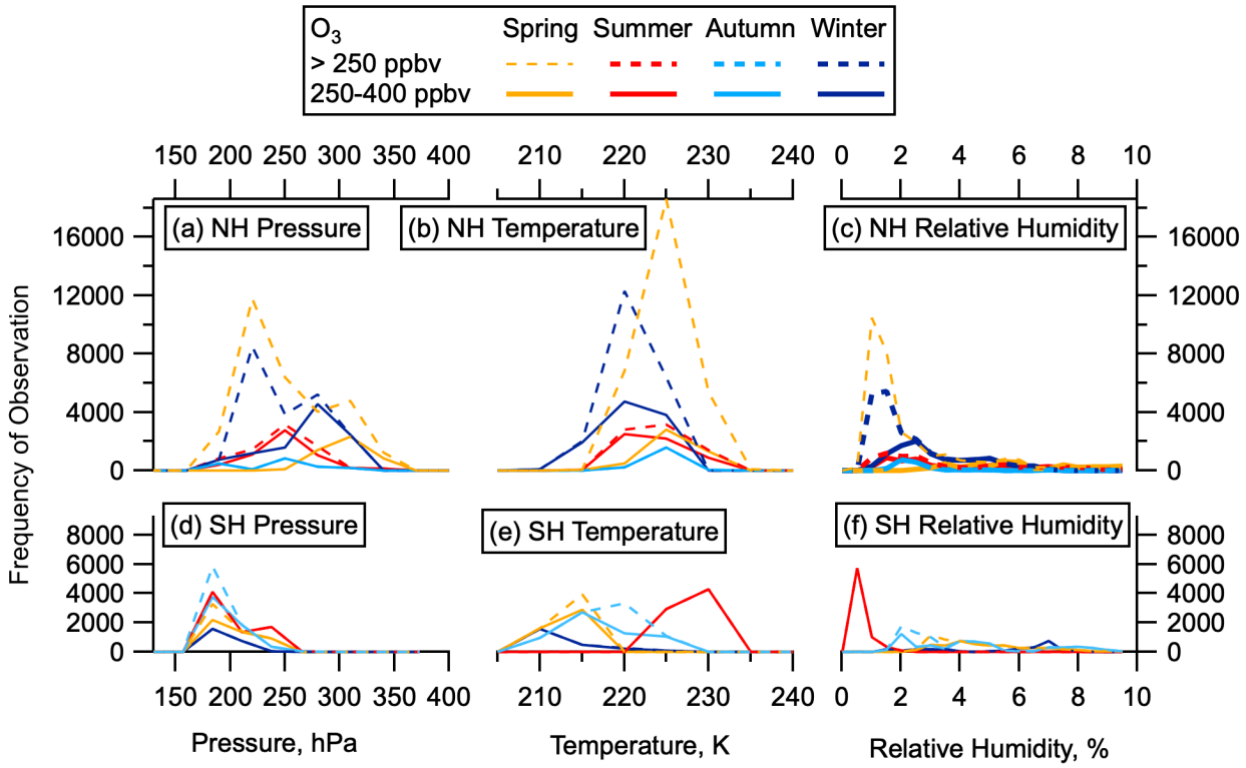

Figure S1: LMS thermodynamic conditions. Histograms of Pressure (a, d), Temperature (b, e) and Relative Humidity (c, f) of observations in the NH and SH LMS respectively (ozone restricted to below 400 ppbv in solid lines).

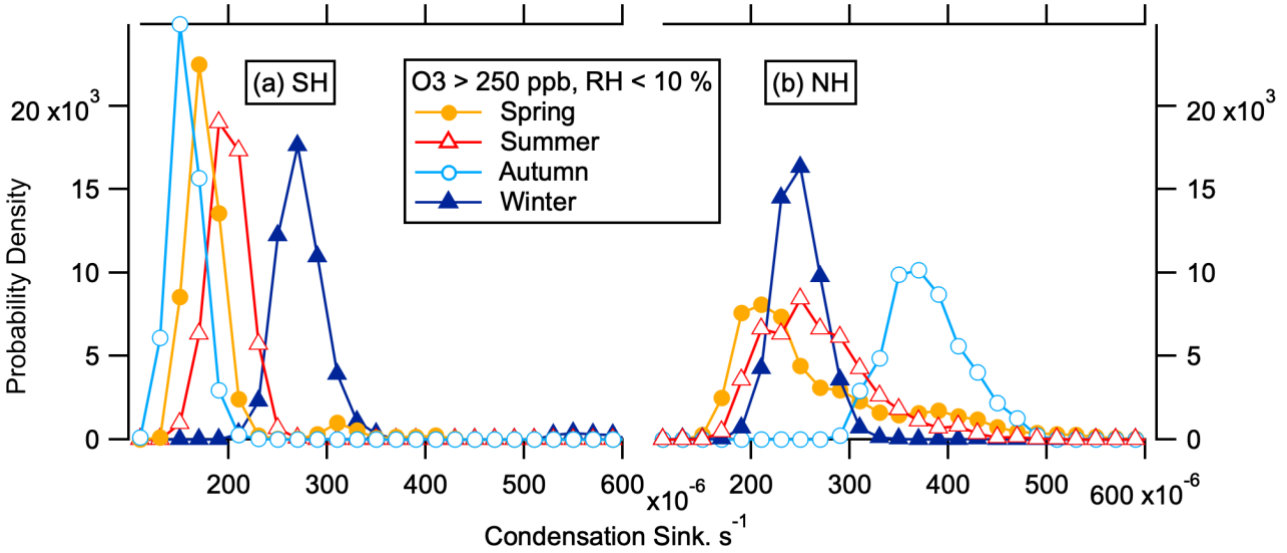

Figure S2: Condensation Sinks in the LMS. Histograms of condensation sinks calculated from size distributions measured in the LMS on ATom in the southern hemisphere (a) and northern hemisphere (b), separated by season.

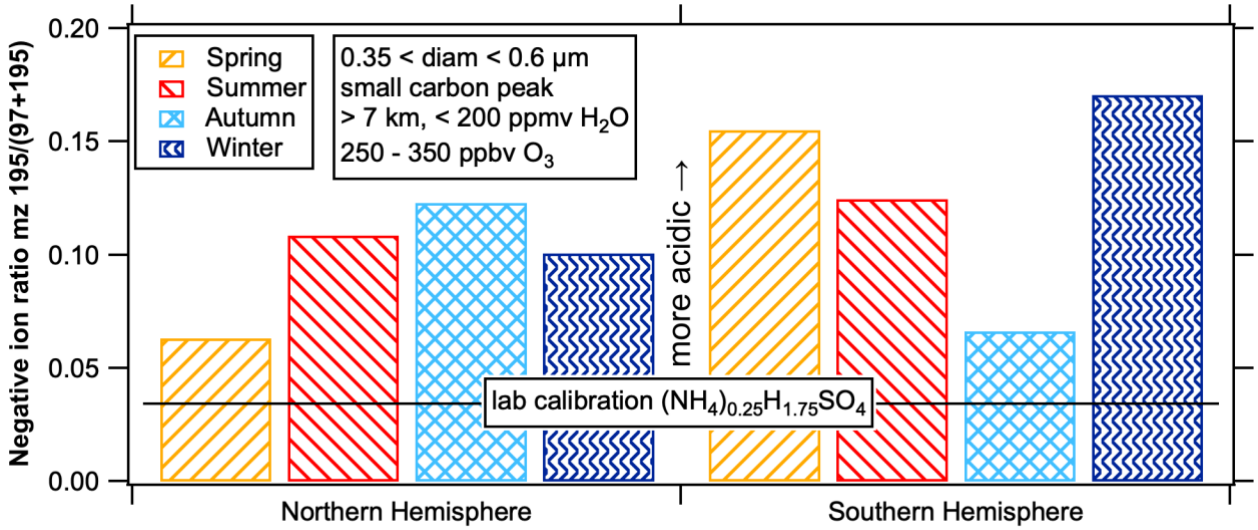

Figure S3: Aerosol acidity in the LMS. Ratio of negative ions of mass to charge ratio (mz) 195 to negative ions of mz (195 + 97) at altitudes > 7 km and water vapour concentrations < 200 ppmv, for the NH (left) and SH (right) separated by season, for particles between 0.35 and 0.6 µm. Lab calibrations of $(NH_4)_{0.25}H_{1.75}SO_4$ clusters had a negative ion ration mz 195/(97+195) of 0.034, therefore we consider ratios higher than this (more acidic) to contain less than 0.25 mole fraction ammonium. Calculations of uptake from the gas phase show that 1 pptv of gas phase ammonia could add 0.25 mol fraction ammonium to sulfuric acid particles in less than a week. The observed acidity sets a limit on the possible concentration of gas phase ammonia.

S2 Particle and SO_2 lifetimes in the LMS

To interpret the small particles and SO_2 enhancements in the NH LMS, it is important to understand both their lifetimes, and also their residence times in the LMS. In winter and spring, seasonal flushing of the LMS limits residence time close to the tropopause to a few weeks. In summer and fall LMS circulation is governed by the monsoons, capping residence times at a few months (Yang et al., 2016;Orbe et al., 2014). The major influence on SO_2 lifetimes in the LMS is reaction with OH. SO_2 lifetime due to reaction with OH in the LMS has been estimated at about 1 month (Höpfner et al., 2015).

For particles, coagulation and growth via condensation are important factors in determining lifetimes at smaller sizes, and sedimentation into the troposphere becomes important at larger sizes. We have calculated coagulation lifetimes of nucleation mode particles with particles large enough that the resulting particle after coagulation is larger than 12 nm (Fig. S4). In the NH LMS these lifetimes range from 9 hours to 3 days in August, February and May, and up to 2.5 weeks in October/ In the SH, due to much lower particle concentration, these lifetimes are on the order of weeks to months.

Growth with respect to sulphuric acid condensation was calculated following the method of Nieminen et al. (2010), giving

$$GR = \frac{C_{SA} \times 2M_{SA} \times cond_K}{\rho \, \pi \, {d_p}^2} \qquad [1]$$

Where C_{SA} is the ambient concentration of sulphuric acid, M_{SA} is the mass of a sulphuric acid molecule, ρ is the density of sulphuric acid in liquid phase (assumed for both the condensing vapour and the particle), and $cond_K$ is in the rate coefficient (cm^3/s) for the condensation of a sulphuric acid molecule on a particle of diameter d_p. This is calculated based on the Fuchs expression for the coagulation rate coefficient following Seinfeld and Pandis (2006).

For 10^5-10^7 cm^{-3} sulphuric acid, we calculate growth rates for nucleation mode particles in the NH LMS conditions ranging from 0.002 nm/h at the 10^5 cm^{-3} sulphuric acid concentrations, 0.024 nm/h at the 10^6 cm^{-3} sulphuric acid concentrations, and 0.3 nm/h at the 10^7 cm^{-3} sulphuric acid concentrations for nucleation mode particles (Fig. S5). While this seems low for growth following a nucleation event compared to common literature values, we note that most prior calculations have been made for boundary layer conditions, and the lower temperatures in the LMS make slower growth rates plausible. Assuming a particle nucleates at around 2 nm, and elevated sulphuric acid concentrations present for 12 hours per day since it is photolytically produced, it would grow out of the nucleation mode through condensation of sulphuric acid only within 1 year, 5 weeks or 3 days, depending on the amount of sulphuric acid. If sulphuric acid levels are low enough to lead to the 1-year or 5-week lifetimes, then coagulation or condensation including HOMS would control the nucleation mode lifetime, and growth from sulphuric acid condensation would not be an important factor.

Highly oxygenated organic molecules (HOMs) contribute to particle growth and formation in a variety of atmospheric environments(Bianchi et al., 2016;Bianchi et al., 2019;Andreae et al., 2018;Tröstl et al., 2016;Zhu et al., 2019). Concentrations of highly oxygenated molecules in the NH LMS as seen on ATom have been estimated to be on the order of pptv(Murphy et al., 2020), and box modelling shows maximum LMS sulfuric acid concentrations from 20 ppb SO_2 of up to around 2 x 10^6 cm^{-3} (Fig. 11). At 300 hPa and 230 K, 1 pptv is equivalent to 10^7 molecules cm^{-3}. Chamber experiments conducted at 248 K at around 1013 hPa with organics but no sulfuric acid, show growth rates from HOM concentrations of 10^7 cm^{-3} of around 1 nm h-1(Stolzenburg et al., 2018). Chamber experiments conducted at sea-level conditions have calculated particle growth rates from concentrations of 10^7 molecules cm^{-3} HOMs and sulfuric acid concentration between 10^4 and 10^6 cm^{-3} to be between 0.2 and 20 nm h^{-1} for 1.1-3.2 nm particles, and between 1 and 10 nm h^{-1} for particles larger than 5 nm(Tröstl et al., 2016). Observed growth rates from the Jungfraujoch High Alpine research station in February (ambient temperatures around 260 K) attributed to 2 x 10^6 cm-3 sulfuric acid were around 0.2 nm h^{-1}, and attributed to around 2 x 10^6 cm^{-3} HOMS were around 0.5 nm h^{-1} (Bianchi et al., 2016), giving a total for HOMs and SA similar to concentrations observed in the LMS of about 0.7 nm h^{-1}, though the temperature on JFJ was around 30 K warmer. If growth is close to the kinetic limit, we do not expect growth rates to vary with pressure, though temperature is likely a factor. While we are not aware of any examples of measured growth rates matching the all of the chemical, temperature and pressure conditions observed in the LMS for nucleation mode aerosol, the above examples indicate that growth rates between 0.2 and 10 nm h^{-1} are reasonable estimates for the NH LMS in the presence of HOMs. Assuming these growth rates are sustained for 12 hours per day (photochemical production of HOMs), this would lead to lifetimes between 1 hour and 4 days.

Growth from sulphuric acid, HOMs and coagulation all interact to determine the lifetime of nucleation mode aerosol in the LMS. Within the large uncertainties of the different processes indicated above, we can conclude that nucleation mode aerosol in the NH LMS have lifetimes on the order of hours to days.

Schroder et al. (2000) showed that despite the higher sinks in aircraft exhaust plume, the effective nucleation mode particle lifetime within the is ~1-2 days because particles are both emitted directly from the engines and form from the gas phase within concentrated and often supersaturated conditions of the plume. Lifetimes of nucleation mode aerosol in the SH LMS are longer than in the NH LMS, since both coagulation sinks and rate of growth out of the nucleation mode are lower due to lower particle and condensable vapour concentrations. However, lifetimes within aircraft plumes will be similar regardless of which hemisphere they are being emitted into, since they are dominated by the production and loss rates in the plume. Therefore, we will assume a 2-day lifetime for nucleation mode particles in the LMS in both hemispheres, and not that this may lead to an underestimate of concentrations in the SH.

Sulphuric acid is produced in the LMS by oxidation of SO2. This occurs in the presence of sunlight, with peak sulphuric acid concentrations occurring near the middle of the day (see Fig. 7). This causes nucleation involving sulphuric acid to occur with a diurnal cycle. No correlation is observed between nucleation mode number concentration and solar zenith angle (Fig. S6) in the NH LMS. This therefore puts a lower limit on the lifetime of nucleation mode aerosol in the NH LMS close to 12 hours.

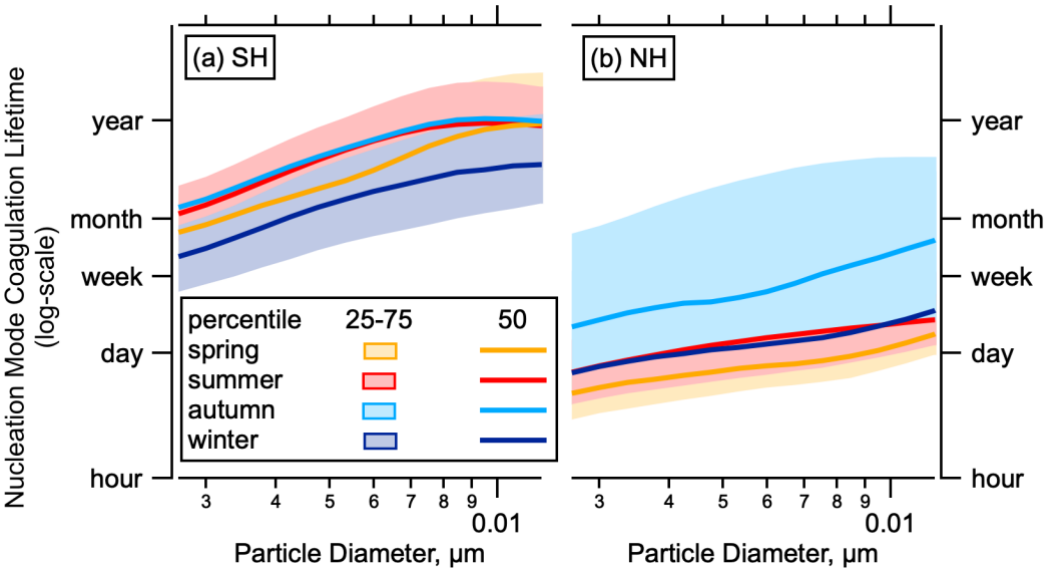

Figure S4: LMS nucleation mode lifetime with respect to coagulation. Calculated median and interquartile range of lifetimes of particles smaller than 12 nm with respect to coagulation that forms particles larger than 12 nm in the LMS (O3 between 250 and 400 ppbv, RH <10 %) in the SH (a) and NH (b) for each season.

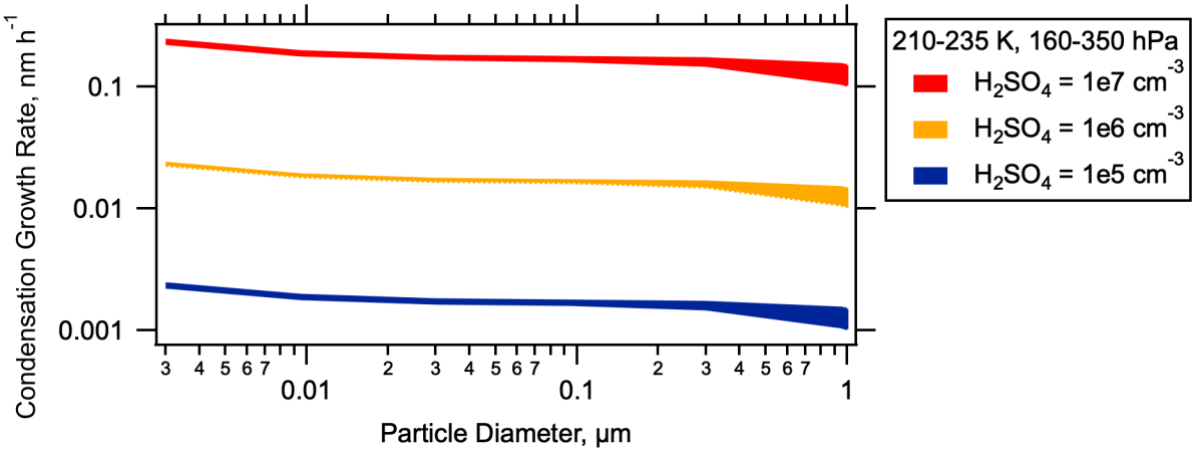

Figure S5: Condensation Growth Rates in the NH LMS. Condensation growth rates as a function of particle diameter, calculated for sulphuric acid (H_2SO_4) concentrations of 10^5, 10^6 and 10^7 cm^{-3} (colours) under NH LMS conditions.

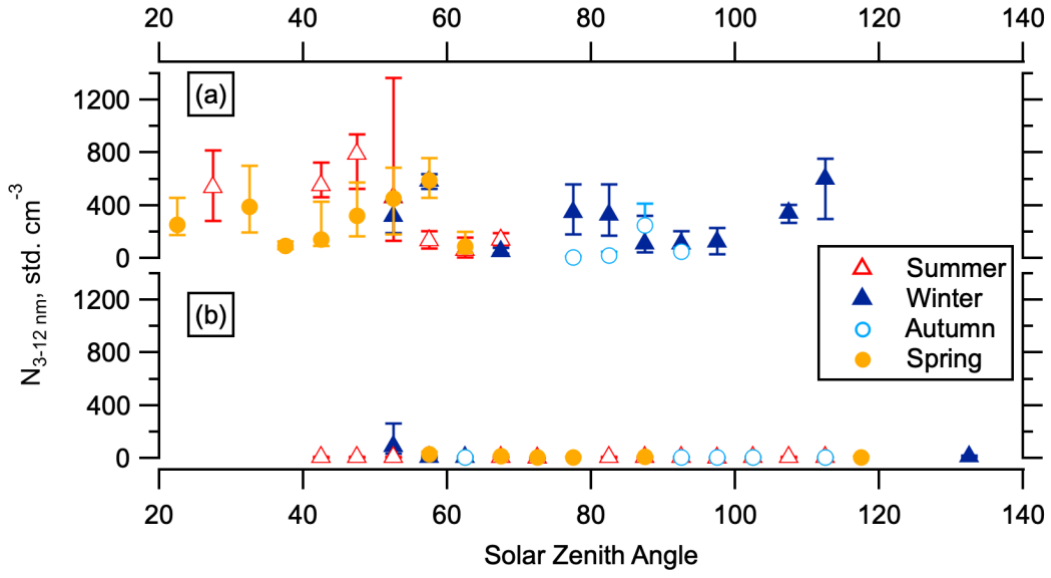

Figure S6: Relationship between nucleation mode number concentration and solar zenith angle in the LMS. Nucleation mode number concentration (50th percentile, with interquartile range given by error bars) as a function of solar zenith angle at time of measurement in the LMS (O_3 > 250 ppbv, RH <10 %) in the NH (a) and SH (b).

S3 Zonal mixing in the LMS

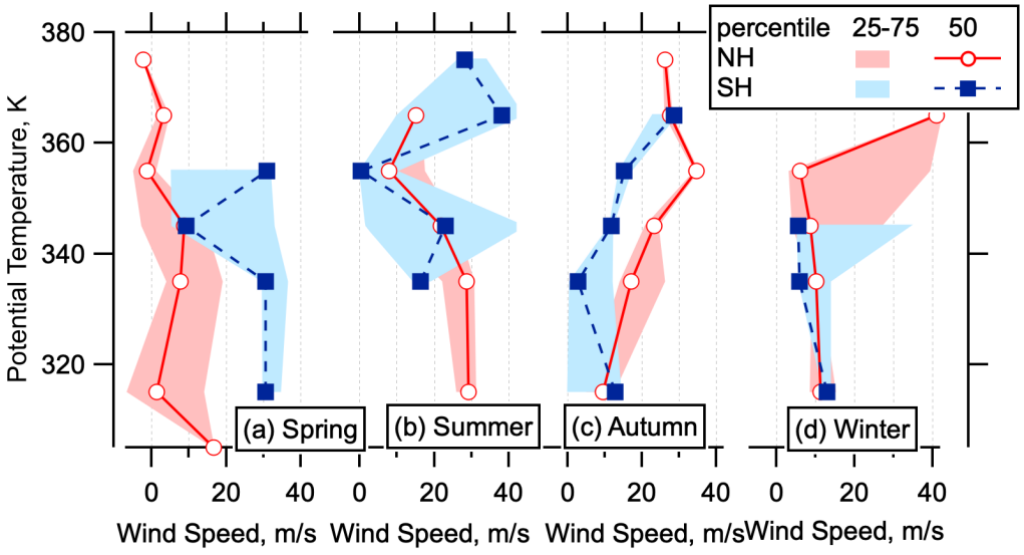

Figure S7: Horizontal windspeeds in the LMS. Horizontal windspeeds encountered on ATom in the LMS by season (a-d) and hemisphere (colours), as a function of potential temperature.

S4 Aviation emissions

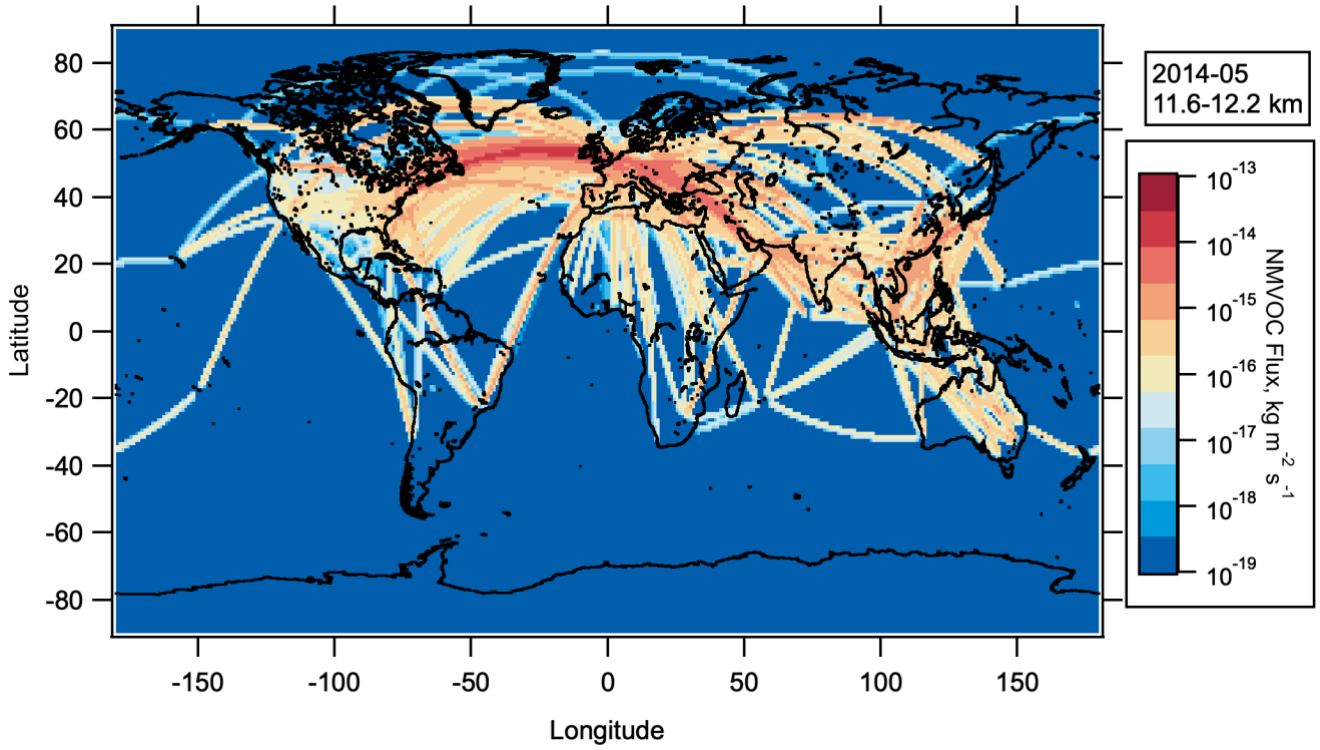

Figure S8: Spatial distribution of NMVOCs emitted by aircraft. NMVOC flux from aircraft from CEDS emissions database for May 2014, between 11.6 and 12.2 km altitude as a function of latitude and longitude. World map was made with Natural Earth Free Vector and Raster Map Data. http://www.naturalearthdata.com (accessed 10 December 2015).

S5. Volcanic Emissions

Table S01: Volcanic activity relevant to ATom LMS observations. Name, latitude, longitude and date of all volcanic eruptions within two months of ATom observations for the four deployments with observed peak emission heights above 7 km altitude. The altitude of the plume height of each eruption, and mass of SO_2 in each plume are given in km and kT respectively. Data are from the Multi-Satellite Volcanic Sulfur Dioxide (SO2) Database Long-Term L4 Global.

* indicates that the plume altitude was was not measured by satellite and instead estimated as a fixed altitude above the vent (10 km for explosive eruptions, 5 km for effusive eruptions).

** indicated that the altitude is estimated as for *, and that even though this estimate lies outside the altitude range we are considering, it is included here because of the larger uncertainty of the emission altitude

volcano	lat	lon	start date	end date	Altitude (km)	SO_2 (kT)	SO_2 NH (kT)	SO_2 SH (kT)
Atom1 29.07.2016 - 23.08.2016						**Total:**	57	0
Etna	37.734	15.004	2016-05-18	2016-05-21	7	5		
Alaid	50.858	155.55	2016-07-04	2016-07-05	7.339*	2		
Kliuchevskoi	56.057	160.638	2016-07-06	2016-08-16	7.5	50		
ATom2 26.01.2017 - 21.02.2017						**Total:**	23.5	2
Chirinkotan	48.98	153.48	2016-11-28	2016-11-28	9	10		
Bogoslof	53.93	-168.03	2016-12-19	2017-01-27	7.6-10.7	10.5		
Fuego	14.473	-90.88	2017-01-26	2017-01-26	7	3		
Piton_de_la_Fournaise	-21.229	55.713	2017-02-01	2017-02-01	7.631*	2		
ATom3 28.09.2017 - 28.10.2017						**Total:**	0	80
Ambae	-15.4	167.83	2017-09-07	2017-09-07	6.496**	40		
Tinakula	-10.38	165.8	2017-10-20	2017-10-20	11	40		
ATom4 24.04.2018 - 21.05.2018						**Total:**	48	153
Fuego	14.473	-90.88	2018-02-01	2018-02-01	7	3		
Sinabung	3.17	98.392	2018-02-19	2018-02-19	17	15		
Kirishimayama	31.934	130.862	2018-03-06	2018-03-07	10	20		
Kirishimayama	31.934	130.862	2018-04-04	2018-04-04	10	10		
Ambae	-15.4	167.83	2018-04-05	2018-04-05	17	150		
Piton_de_la_Fournaise	-21.229	55.713	2018-04-28	2018-04-28	7.631*	3		

References

Andreae, M. O., Afchine, A., Albrecht, R., Holanda, B. A., Artaxo, P., Barbosa, H. M. J., Borrmann, S., Cecchini, M. A., Costa, A., Dollner, M., Futterer, D., Jarvinen, E., Jurkat, T., Klimach, T., Konemann, T., Knote, C., Kramer, M., Krisna, T., Machado, L. A. T., Mertes, S., Minikin, A., Pohlker, C., Pohlker, M. L., Poschl, U., Rosenfeld, D., Sauer, D., Schlager, H., Schnaiter, M., Schneider, J., Schulz, C., Spanu, A., Sperling, V. B., Voigt, C., Walser, A., Wang, J., Weinzierl, B., Wendisch, M., and Ziereis, H.: Aerosol characteristics and particle production in the upper troposphere over the Amazon Basin, Atmos Chem Phys, 18, 921-961, 10.5194/acp-18-921-2018, 2018.

Bianchi, F., Trostl, J., Junninen, H., Frege, C., Henne, S., Hoyle, C. R., Molteni, U., Herrmann, E., Adamov, A., Bukowiecki, N., Chen, X., Duplissy, J., Gysel, M., Hutterli, M., Kangasluoma, J., Kontkanen, J., Kurten, A., Manninen, H. E., Munch, S.,

Perakyla, O., Petaja, T., Rondo, L., Williamson, C., Weingartner, E., Curtius, J., Worsnop, D. R., Kulmala, M., Dommen, J., and Baltensperger, U.: New particle formation in the free troposphere: A question of chemistry and timing, Science, 352, 1109-1112, 10.1126/science.aad5456, 2016.

Bianchi, F., Kurtén, T., Riva, M., Mohr, C., Rissanen, M. P., Roldin, P., Berndt, T., Crounse, J. D., Wennberg, P. O., Mentel, T. F., Wildt, J., Junninen, H., Jokinen, T., Kulmala, M., Worsnop, D. R., Thornton, J. A., Donahue, N., Kjaergaard, H. G., and Ehn, M.: Highly Oxygenated Organic Molecules (HOM) from Gas-Phase Autoxidation Involving Peroxy Radicals: A Key Contributor to Atmospheric Aerosol, Chem. Rev., 119, 3472-3509, 10.1021/acs.chemrev.8b00395, 2019.

Höpfner, M., Boone, C. D., Funke, B., Glatthor, N., Grabowski, U., Günther, A., Kellmann, S., Kiefer, M., Linden, A., Lossow, S., Pumphrey, H. C., Read, W. G., Roiger, A., Stiller, G., Schlager, H., von Clarmann, T., and Wissmüller, K.: Sulfur dioxide (SO₂) from MIPAS in the upper troposphere and lower stratosphere 2002–2012, Atmos. Chem. Phys., 15, 7017-7037, 10.5194/acp-15-7017-2015, 2015.

Murphy, D. M., Froyd, K. D., Bourgeois, I., Brock, C. A., Kupc, A., Peischl, J., Schill, G. P., Thompson, C. R., Williamson, C. J., and Yu, P.: Radiative and chemical implications of the size and composition of aerosol particles in the existing or modified global stratosphere, Atmos. Chem. Phys. Discuss., 2020, 1-32, 10.5194/acp-2020-909, 2020.

Nieminen, T., Lehtinen, K. E. J., and Kulmala, M.: Sub-10 nm particle growth by vapor condensation – effects of vapor molecule size and particle thermal speed, Atmos. Chem. Phys., 10, 9773-9779, 10.5194/acp-10-9773-2010, 2010.

Orbe, C., Holzer, M., Polvani, L. M., Waugh, D. W., Li, F., Oman, L. D., and Newman, P. A.: Seasonal ventilation of the stratosphere: Robust diagnostics from one-way flux distributions, Journal of Geophysical Research: Atmospheres, 119, 293-306, https://doi.org/10.1002/2013JD020213, 2014.

Schroder, F., Brock, C. A., Baumann, R., Petzold, A., Busen, R., Schulte, P., and Fiebig, M.: In situ studies on volatile jet exhaust particle emissions: Impact of fuel sulfur content and environmental conditions on nuclei mode aerosols, J Geophys Res-Atmos, 105, 19941-19954, Doi 10.1029/2000jd900112, 2000.

Seinfeld, J. H., and Pandis, S. N.: Atmospheric chemistry and physics from air pollution to climate change, 2nd ed., Wiley, Hoboken, N.J., 1203 S. pp., 2006.

Stolzenburg, D., Fischer, L., Vogel, A. L., Heinritzi, M., Schervish, M., Simon, M., Wagner, A. C., Dada, L., Ahonen, L. R., Amorim, A., Baccarini, A., Bauer, P. S., Baumgartner, B., Bergen, A., Bianchi, F., Breitenlechner, M., Brilke, S., Mazon, S. B., Chen, D. X., Dias, A., Draper, D. C., Duplissy, J., Haddad, I., Finkenzeller, H., Frege, C., Fuchs, C., Garmash, O., Gordon, H., He, X., Helm, J., Hofbauer, V., Hoyle, C. R., Kim, C., Kirkby, J., Kontkanen, J., Kuerten, A., Lampilahti, J., Lawler, M.,

Lehtipalo, K., Leiminger, M., Mai, H., Mathot, S., Mentler, B., Molteni, U., Nie, W., Nieminen, T., Nowak, J. B., Ojdanic, A., Onnela, A., Passananti, M., Petaja, T., Quelever, L. L. J., Rissanen, M. P., Sarnela, N., Schallhart, S., Tauber, C., Tome, A., Wagner, R., Wang, M., Weitz, L., Wimmer, D., Xiao, M., Yan, C., Ye, P., Zha, Q., Baltensperger, U., Curtius, J., Dommen, J., Flagan, R. C., Kulmala, M., Smith, J. N., Worsnop, D. R., Hansel, A., Donahue, N. M., and Winkler, P. M.: Rapid growth of organic aerosol nanoparticles over a wide tropospheric temperature range, Proc. Natl. Acad. Sci. U.S.A., 115, 9122-9127, 10.1073/pnas.1807604115, 2018.

Tröstl, J., Chuang, W. K., Gordon, H., Heinritzi, M., Yan, C., Molteni, U., Ahlm, L., Frege, C., Bianchi, F., Wagner, R., Simon, M., Lehtipalo, K., Williamson, C., Craven, J. S., Duplissy, J., Adamov, A., Almeida, J., Bernhammer, A.-K., Breitenlechner, M., Brilke, S., Dias, A., Ehrhart, S., Flagan, R. C., Franchin, A., Fuchs, C., Guida, R., Gysel, M., Hansel, A., Hoyle, C. R., Jokinen, T., Junninen, H., Kangasluoma, J., Keskinen, H., Kim, J., Krapf, M., Kürten, A., Laaksonen, A., Lawler, M., Leiminger, M., Mathot, S., Möhler, O., Nieminen, T., Onnela, A., Petäjä, T., Piel, F. M., Miettinen, P., Rissanen, M. P., Rondo, L., Sarnela, N., Schobesberger, S., Sengupta, K., Sipilä, M., Smith, J. N., Steiner, G., Tomè, A., Virtanen, A., Wagner, A. C., Weingartner, E., Wimmer, D., Winkler, P. M., Ye, P., Carslaw, K. S., Curtius, J., Dommen, J., Kirkby, J., Kulmala, M., Riipinen, I., Worsnop, D. R., Donahue, N. M., and Baltensperger, U.: The role of low-volatility organic compounds in initial particle growth in the atmosphere, Nature, 533, 527-531, 10.1038/nature18271, 2016.

Yang, H., Chen, G., Tang, Q., and Hess, P.: Quantifying isentropic stratosphere-troposphere exchange of ozone, Journal of Geophysical Research: Atmospheres, 121, 3372-3387, 10.1002/2015jd024180, 2016.

Zhu, J., Penner, J. E., Yu, F., Sillman, S., Andreae, M. O., and Coe, H.: Decrease in radiative forcing by organic aerosol nucleation, climate, and land use change, Nat Commun, 10, 423-423, 10.1038/s41467-019-08407-7, 2019.